Generalized Electrical Substitution Methods and Detectors for Absolute Optical Power Measurements

S.I. Woods[1], J.E. Neira[2], J.E. Proctor[2], J.P. Rice[1],
N.A. Tomlin[3], M.G. White[3,4], M.S. Stephens[3] and J.H. Lehman[3]

[1]*National Institute of Standards and Technology (NIST), Gaithersburg, MD 20899, USA*
[2]*Jung Research and Development Corp., Bethesda, MD 20816 USA*
[3]*National Institute of Standards and Technology (NIST), Boulder, CO 80305, USA*
[4]*Department of Physics, University of Colorado, Boulder, Colorado 80309, USA*

Corresponding e-mail address: solomon.woods@nist.gov

Abstract

We have developed generalized methods for electrical substitution optical measurements, as well as cryogenic detectors which can be used to implement them. The new methods detailed here enable measurement of arbitrary periodic waveforms by an electrical substitution radiometer (ESR), which means that spectral and dynamic optical power can be absolutely calibrated directly by a primary standard detector. Cryogenic ESRs are not often used directly by researchers for optical calibrations due to their slow response times and cumbersome operation. We describe two types of ESRs with fast response times, including newly developed cryogenic bolometers with carbon nanotube absorbers, which are manufacturable by standard microfabrication techniques. These detectors have response times near 10 ms, spectral coverage from the ultraviolet to far-infrared, and are ideal for use with generalized electrical substitution. In our first tests of the generalized electrical substitution method with FTS, we have achieved uncertainty in detector response of 0.13 % (k=1) and total measurement uncertainty of 1.1 % (k=1) in the mid-infrared for spectral detector responsivity calibrations. The generalized method and fast detectors greatly expand the range of optical power calibrations which can be made using a wideband primary standard detector, which can shorten calibration chains and improve uncertainties.

1. Introduction

The electrical substitution (ES) technique has been used for over a century to quantify optical power [1,2], and for more than 40 years absolute optical detectors have employed electrical substitution to define a detector-based optical scale [3-6]. Despite its long history, the ES technique has been used only for a very narrow range of measurement configurations, essentially limiting its direct application to calibrations of constant or slowly chopped optical radiation. We describe a generalization of the ES method, which relies upon the high-speed capabilities of modern digital electronics, that will enable direct quantification of diverse optical signals by a primary standard detector.

1.1. Absolute Cryogenic Radiometers (ACRs)

The absolute electrical substitution radiometer (ESR) is an electrically-substituted radiometer which incorporates a receiver with near-unity absorption. By converting nearly all incident optical radiation into heating of the thermally-isolated receiver and integrating a thermometer and electrical heater with it, a close equivalence between the incident optical power and the electrical power delivered to the receiver is realized. In this way, optical power is

traceable through the measurement of electrical voltage and resistance, two quantities which can be calibrated with very low uncertainties [7,8]. In this work, we will concentrate on describing how electrical substitution expands the capability of this type of bolometric detector and how to extend the scope of electrical substitution to any periodic optical input signal. Cooling an absolute ESR to liquid helium temperature makes it possible to significantly lower its noise, increase its speed, and lower detector optical/electrical non-equivalence. This cryogenic version, known as an absolute cryogenic radiometer (ACR), has been a staple for low uncertainty optical calibrations for more than 30 years [9-12].

1.2. Time Constants and ES Techniques

To date, applications of ACRs have been typically limited to constant optical signals or relatively slow, well-chopped signals (nearly square wave or sinusoidal). Thermal time constants for ACRs have historically been relatively long, from 1 s to 200 s, but they don't have to be. The long time constants have been driven by the need to absorb nearly all the incident light, which is most readily accomplished by engineering the receiver as a light-trapping cavity with significant thermal inertia. A faster design, the electrically-substituted bolometer (ESB), however, has more recently exploited highly absorbing films such as gold-black [13] or vertically-aligned carbon nanotubes [14] to accomplish near-unity absorption over a broad spectral range using a thin film structure on a planar receiver. Time constants have already been reduced to about 10 ms, and further reductions are possible with further miniaturization and use of substrates made from membranes. A more general electrical substitution method can exploit these faster ACRs to quantify arbitrary optical pulse trains, and even transient signals, at higher frequencies. In turn, the increased measurement flexibility enabled by generalized electrical substitution will motivate accelerated development of higher speed ACRs.

Phase sensitive or lock-in techniques have been successfully used with electrical substitution detectors, and procedures developed in these studies can be built upon to enable feedback control for arbitrary optical pulse trains. An early primary standard detector developed with electrical substitution of chopped signal was the electrically-calibrated pyroelectric radiometer (ECPR). Pyroelectric detectors are only sensitive to changing optical inputs, so this radiometer used a chopper at 17 Hz, lock-in detection, and an analog nulling circuit which compared optical and electrical signals on the pyroelectric element [15]. Even though traditional ACRs are even slower than pyroelectric detectors, digital phase-sensitive detection has been used over long time scales to achieve higher signal-to-noise [16]. Most electrical-substitution radiometers are operated in "closed loop" mode, where feedback is used to balance optical and electrical heating of the receiver, resulting in zero net temperature change at a thermometer located on the receiver. There is a feedback time constant associated with this nulling of the signal, which will be larger than the thermal detection time constant, often by a margin of 100 % or more. The so-called feedforward method has been successfully used with ACRs to decrease the feedback time constant: if the optical power in a signal can be estimated before the ACR measurement, this change in electrical power can be used as the initial starting point for the nulling procedure, significantly reducing the time until temperature stabilization. The

feedforward concept will be used in a slightly different form in our generalized substitution procedure.

1.3. Response Linearization

In addition to providing an absolute scale for optical power, electrical substitution also has the important effect of "linearizing" the response of a bolometer over a greatly expanded optical power range. The bolometer is an intrinsically non-linear device because both the

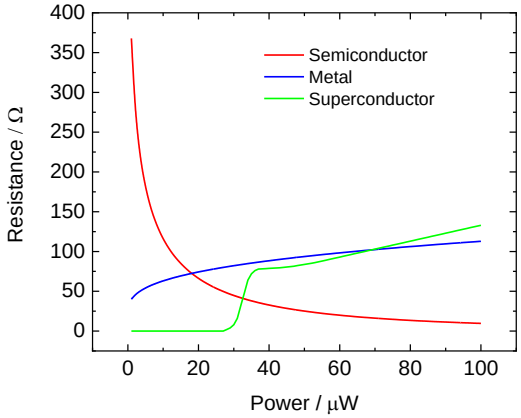

Figure 1. Typical resistance-power response curves for different types of thermistors used as part of a bolometer.

dependence of temperature on power and the dependence of the thermometer resistance (typically a thermistor is used) on temperature are not generally linear, and neither is their product. Figure 1 shows typical response curves for a few different absorber and thermometer materials. Only for small changes in power can the response (typically the voltage across a resistor for a fixed current) be approximated as linear. Using electrical substitution, however, the

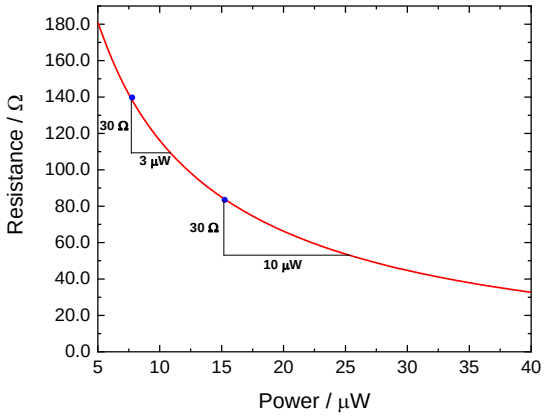

Figure 2. Change of resistance with power can be strongly dependent on starting resistance for a bolometer. For instance, the same 30 Ω change in resistance is induced by power changes different by a factor of more than 3 in the plot above.

ultimate measurand (i.e., the measured electrical power) is equivalent to the optical power, so is by default linear over the full range where the detector can be operated. It is also important to note that a bolometer generally has a very large direct current (DC) null signal; i.e., in the absence of optical signal the resistance of the bolometer is large compared to the resistance change which would be induced by the optical signal. This means that any absolute measurement with a bolometer needs to measure background response, so must be equivalent to either a shuttered DC measurement or chopped alternating current (AC) measurement which quantifies response differences in real time. Bolometer response (resistance) is not a one-to-one function of applied power (optical or electrical), unless the resistance with no applied power is also specified. Figure 2 illustrates how the same resistance change can be induced by two different power changes, and so the starting resistance must be precisely quantified. It may seem that electrical substitution introduces extraneous complications in the measurement of a bolometer, but in fact due to non-linearity and large null signal, it is always necessary to make two measurements (equivalent to signal and background) on a bolometer to precisely quantify response, whether electrical substitution is used or not.

1.4. Impact of Generalized ES

With generalized electrical substitution, ACRs can be readily used with Fourier-transform spectrometers (FTS) for absolute spectral calibrations. Fourier-transform infrared (FTIR) spectroscopy requires linear detector response, and the time constants of gold-black ESBs and planar bolometric radiometers (PBRs) are compatible with continuous-scan FTIR. Historically, given the slow speeds of ACRs, they have been used almost exclusively by national metrological institutes (NMIs) to calibrate secondary reference standard detectors which are faster and easier to operate. Generalized electrical substitution opens up the possibility of removing the secondary reference standard from the traceability chain for many applications, enabling researchers to employ a primary standard detector directly for absolute broadband and spectral measurements. Secondary reference standards are often only calibrated by ACRs at a few spectral tie points by NMIs, but researchers could directly use ACRs with generalized ES to calibrate their own systems at the wavelengths and power levels where they typically operate. Armed only with a calibrated voltmeter and resistor, researchers could maintain their optical power traceability to the SI within the “in situ” conditions of their laboratory equipment. The first types of measurements we have performed using generalized electrical substitution with FTS are for spectral detector responsivity calibrations. It is also possible to use this technique for spectral source calibrations and optical system spectral throughput calibrations, but these measurements require an additional step where the spectral throughput of the FTS is first calibrated using a standard reference source.

2. Existing Electrical Substitution Techniques

We will begin by outlining existing techniques for electrical substitution in order to facilitate the discussion of our generalized method.

2.1. ESR Design and DC Measurements

The components of an absolute electrical substitution radiometer (an ACR in the cryogenic case) are shown in Figure 3. Light is incident upon an absorber, which is designed to absorb nearly all incident optical radiation within some broad wavelength band. The absorber is

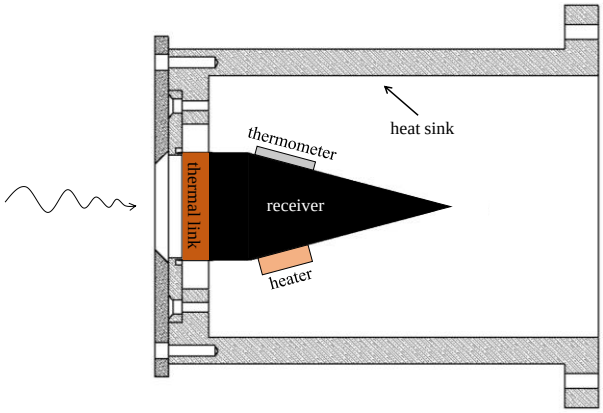

Figure 3. Schematic depicting the key components of a cryogenic electrical substitution radiometer, also known as an ACR.

located on the receiver structure; traditionally the receiver has been a light-trapping structure such as a cone to achieve high enough absorptivity, but for PBRs with vertically-aligned carbon nanotubes can be a simple substrate or membrane. The receiver is attached by a thermal link to a temperature-controlled heat sink, which provides a stable heat reservoir for the receiver. Thermal link thermal conductivity is specifically chosen to achieve a particular thermal time constant and detector sensitivity. A heater and thermometer on the receiver are used in a proportional-integral-derivative (PID) control loop to maintain the receiver at a fixed temperature, making electrical substitution possible. Operating an ACR at a fixed receiver temperature is known as "closed loop" mode and operating without temperature control at a fixed heater power is known as "open loop." The electrical power is monitored using a 4-wire measurement of current and voltage to the ACR heater. One voltmeter monitors the voltage across the heater, and a second voltmeter monitors the voltage across a calibrated series resistor to measure the current flowing through the heater. The applied electrical heater power, given by the current-voltage product, is constantly logged.

Electrical substitution for constant optical signals is the most common ES configuration, and depends upon a simple nulling method. First, a shutter is used to block all signal from the optical source to the receiver. The receiver is controlled at a high enough temperature so that when the shutter is open it will still be possible to reach this temperature by lowering the power to the electrical heater. Practically speaking, this means that the heater power applied when the shutter is closed should be larger than the expected optical power from the source. A time trace of the general procedure is shown in Figure 4. The total power applied (optical + electrical) to the receiver is always the same, so receiver temperature is constant. Here we assume the heat sink temperature is also constant. During half the time (shutter closed) the total power (P_{tot}) is all supplied by the heater and during the other half (shutter open) the heater only supplies the part of the total (P_{tot} - P_{opt}) not supplied by the optical signal (P_{opt}). There is a transition time between

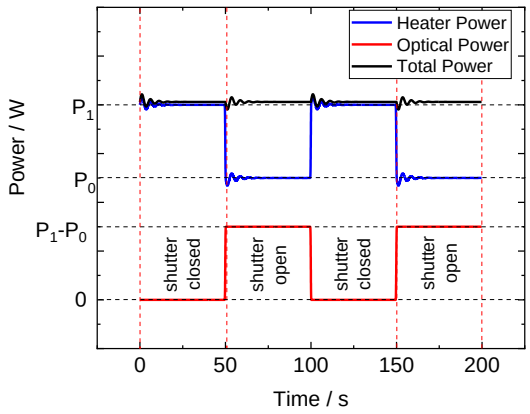

Figure 4. Schematic of electrical and optical power traces in standard DC electrical substitution. The total power applied to the receiver is kept constant via temperature control and is divided between contributions from the optical source and the electrical heater.

the shutter closed and shutter open measurement during which the heater power is evolving under the influence of the PID control loop in order to maintain a fixed temperature. Detector response is determined by waiting long enough between cycles to define a series of stable plateaus: the response recorded is the heater power difference between the open and closed shutter positions (P_{opt}). By using statistics (multiple measurements on each plateau or many plateau cycles) it is possible to achieve power uncertainties an order of magnitude lower than power fluctuations of the stable state. A nearly ideal ACR will have a low "non-equivalence" between its electrical and optical heating: this will follow if the total heat flow from the receiver (heat flow to the heat sink and radiative losses) is identical under conditions of electrical or optical heating, if the optical absorptance of the ACR is near unity, and if electrical power is dissipated almost exclusively at the heater (as opposed to along the heater leads). Often the level of non-equivalence is quantified by attaching two different heaters at different locations on the receiver. The same electrical power is applied to each heater in turn, and the agreement between receiver temperature change for the two cases is measured.

2.2. AC Chopped Measurements

2.2.1. Standard ES Procedures

A number of possible methods exist to perform electrical substitution on chopped AC (approximately square wave) or electro-optically modulated (sinusoidal) signals, and we will want to build upon a method most readily extended to high frequencies for our generalized ES. In the discussion below we will concentrate on chopped, approximately square wave signals with 50 % duty cycle, but the methods developed will apply equally well to approximately sinusoidal optical signals. In all cases, to operate in AC mode the thermal time constant (τ_{therm}) of the ACR must be comparable to the chopping period or shorter, i.e., $\tau_{therm} \le \tau_{chop} = 1/f_{chop}$. If $\tau_{therm} \gg \tau_{chop}$, then the ACR will not have sufficient time to respond to signal changes, and response will be

near zero. In the limit $\tau_{therm} \ll \tau_{chop}$, the ACR will have enough time to change and plateau during each chopping cycle, just as in the DC shuttered ES method.

The first AC chopped method is simply the same as the DC method, and is available in the case where the effective PID feedback time constant τ_{fb} can also be kept smaller than τ_{chop}. In other words, if chopping is slow enough relative to the PID loop feedback, then the chopped case looks exactly like the shutter-open/shutter-closed case. The feedback time constant τ_{fb} is usually at least several times larger than τ_{therm} and there are significant limitations to the speed of commercial temperature controllers, so this method is typically only viable up to a frequency of about 10 Hz. It is therefore not readily generalized to higher frequencies as we require.

The second AC chopped method works well in the case where the optical signal is nearly a perfect square wave, and uses a lock-in technique to perform PID feedback nulling of the sum of the amplitudes of the optical and electrical signals. The goal here is to generate an electrical heater power square pulse with just the right amplitude and phase to exactly cancel the optical chopper signal. This version of AC chopped electrical substitution has been developed fully for use with the electrically-calibrated pyroelectric radiometer (ECPR) for absolute power measurements [3,4,15]. Optical and electrical power square waves are applied to the detector at the same time and the fundamental frequency of the thermometer response is monitored by a lock-in amplifier. The phase and frequency of the optical and electrical signals are matched by using the sync signal from the chopper, which is provided by a photodetector monitoring the chopper blade. The optical and electrical signals can be tested separately so that any slight deviations in phase matching due to imperfections in the synchronization method can be reduced by introducing time delay for the electrical signal triggering. The lock-in output is used as the input for a PID feedback loop to set the correct amplitude for the electrical heater signal. When the optical and electrical signals have equal amplitude and are 180° out of phase, they will most nearly null the receiver temperature variations, and the feedback loop will stabilize at the correct electrical power. As described before, the current and voltage applied to the heater are constantly monitored, so RMS heater electrical power can be readily computed for the current-voltage product.

In the original ECPR experiments an analog PID loop was used, but it is now possible to execute the nulling procedure using digital signal processing. In this technique, PID control is not performed within each chopper cycle (as is required in the pseudo-DC method) but rather on the average amplitude of the square waves, so τ_{fb} can be significantly larger than τ_{chop}. This allows lock-in PID nulling to be effective for much higher frequencies, but this method is not readily generalizable to arbitrary signals. It depends on an assumption about the optical waveform (near ideal square wave) which will not in general be true, and it cannot be multiplexed over more than one frequency at a time.

Before pursuing a method which can be easily multiplexed, let us consider some common causes of non-ideal square wave character in chopped signals. If the optical beam diameter (d_{beam}) is significant in size compared to the chopper opening ($w_{opening}$), the square wave will develop slanted walls as shown in Figure 5. As long as $d_{beam} \ll w_{opening}$, a significant plateau

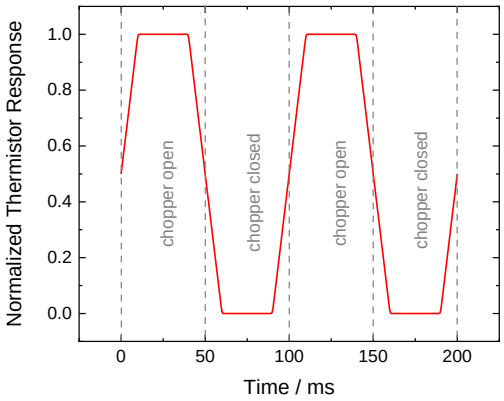

Figure 5. Characteristic waveform of the optical signal from a chopped source when the size of the beam is a significant fraction of the chopper opening distance.

region will exist for correctly quantifying the optical power amplitude. If the detector time constant is a significant fraction of the chopper period, then the leading edge of the square wave will be curved by the heating saturation curve as plotted in Figure 6. A significant plateau region will exist as long as $\tau_{therm} \ll \tau_{chop}$. The differential equation which governs the time evolution of the detector temperature is nearly identical to that for an electrical circuit with passive components (e.g. RL circuit), so the heating/cooling curve in response to a square wave closely resembles the analogous effect of charging/discharging in an electrical circuit with passive components. Geometrical and mechanical imperfections in the chopper can also lead to departure from perfect square wave behavior. If the lobes of the chopper wheel are slightly

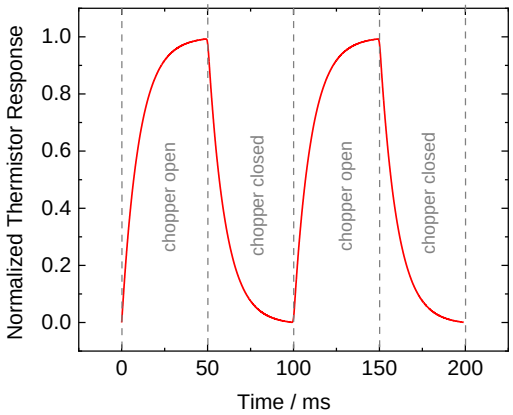

Figure 6. Characteristic response of an ACR to the optical signal from a chopped source when the ACR thermal relaxation time (τ_{therm}) is 5 times shorter than the chopper period (τ_{chop}).

different sizes, adjacent square wave pulses will have slightly different durations. Likewise, a chopper which has non-uniformities in angular velocity will exhibit phase jitter and non-uniform pulse durations. All these sources of square wave imperfection will lead to error in the basic lock-in PID-nulling method. It will not be possible to completely cancel the optical signal with an electrical square wave feedback, and there will be uncertainty added to the phase and period of the optical signal. If the thermal time constant is not much shorter than the chopper period, then there will be more uncertainty and systematic error associated with the correct power amplitude.

2.2.2. Iterative Feedforward Procedure

We will next describe an AC-chopped ES method which may appear more primitive than the lock-in PID-nulling method, but has the advantage that the feedforward and final measurement steps are separated, facilitating higher speed measurements and frequency when modified for use with an FTS. This method couples an iterative nulling feedback step on test pulses, followed by a measurement step in which a feedforward electrical signal is applied to mostly cancel net power on the detector. The measurement step is made open loop, but the signal is driven to nearly zero by the applied feedforward power, so the bolometer is well within its linear regime and there is little error associated with a linear estimate of power from the resistance change. The iterative feedforward procedure contains the following specific steps:

1) <u>*Test Waveform Heater Signal:*</u> With optical signal blocked, apply square wave test pulses of known power to the detector heater and record amplitude and phase of the detector thermometer response. Denote by $\Delta H_{test}(t)$ the applied heat pulse differential power, by $\Delta R_{test}(t)$ the resistive change response of the thermometer and by $\Delta\varphi_h$ the phase delay between the response and the drive signal. The amplitude of the applied heat pulse is denoted by H_o, and the amplitude of the resistive change of the thermometer in response is R_o. Denote by $f_h(t)$ the time-dependent shape of the applied heat pulse and by $f_r(t)$ the time-dependent shape of the resistive change response. As discussed earlier, the shape of $\Delta R_{test}(t)$ will in general be deformed from square wave by the bolometer time constant, and will also be delayed by a time $\Delta\varphi_h/\omega_o$ relative to the heater drive, where ω_o is the angular frequency (equal to 2π/T, where T is the period) shared by the heater drive and thermometer response. We can write:

$$\Delta H_{test}(t) = H_o f_h(t) \text{ , where } f_h(t+\frac{2\pi}{\omega_o}) = f_h(t) \qquad (1)$$

$$\Delta R_{test}(t) = R_o f_r(t-\frac{\Delta\varphi_h}{\omega_o}) \text{ , where } f_r(t+\frac{2\pi}{\omega_o}) = f_r(t)$$

2) <u>*Open Loop Optical Signal:*</u> Let chopped optical signal reach the detector, and then measure the thermometer response (with no electrical power applied to the heater). Denote measured thermometer response to the optical signal by $\Delta R_{opt}(t)$, where:

$$\Delta R_{opt}(t) = L_o f_L(t - \frac{\Delta\varphi_L}{\omega_o}) \text{ , where } f_L(t + \frac{2\pi}{\omega_o}) = f_L(t) \qquad (2)$$

$\Delta R_{opt}(t)$ will be deformed from square wave by the bolometer time constant and chopper effects, and will also be delayed by a time $\Delta\varphi_L/\omega_o$ relative to the chopper. The same frequency should be used for the chopper and heater test pulses, and $\Delta\varphi_L/\omega_o \approx \Delta\varphi_h/\omega_o$. The amplitude of the response to light is denoted by L_o and the shape of the resistive change response is $f_L(t)$.

3) <u>*First Estimate for Nulling:*</u> Use a linear approximation for heater power based on the test signal response, and use difference of phase between test and optical signals. To estimate how much heater power would be required to achieve a response equal to the optical signal, scale the test pulse amplitude by the ratio of optical/test responses. Therefore, the first estimate of the nulling signal from the heater is:

$$\Delta H_1(t) = -L_o \frac{H_o}{R_o} f_h(t - \frac{\Delta\varphi_L}{\omega_o} + \frac{\Delta\varphi_h}{\omega_o}) \qquad (3)$$

where the phase is defined relative to the chopper synchronization signal, and the leading negative sign on the righthand side is needed because the nulling signal from the heater must be 180° out-of-phase to cancel the optical signal. In this linear approximation, the ratio between drive and response is always given by the local two-point slope of the resistance-power response curve. The first estimate will be most accurate for very small optical signals, but if the response has significant non-linearity, an iterative procedure will be used to null the signal. If delays associated with heating and readout are the same for optical and electrical inputs, then the time shift $\Delta\varphi_L/\omega_o - \Delta\varphi_h/\omega_o$ will only be that associated with the chopper sync signal to chopper blade edge delay.

4) <u>*Response with Nulling Applied:*</u> The heater signal $\Delta H_1(t)$ from Eq. (3) is now applied together with the optical signal, and the net response from the thermometer is measured. The response is the first error signal, the difference between the first approximation for nulling and the measured result. Denote thermistor response to the electrical heater signal $\Delta H_1(t)$ as $\Delta R_1(t)$, where $\Delta R_1(t) = R_1 f_r(t)$ and it will partially cancel the optical signal. The total error signal at the bolometer will be:

$$\Delta R_{err1}(t) = \Delta R_{opt}(t) + \Delta R_1(t) \qquad (4)$$

5) <u>*Continue Iterating:*</u> If $\Delta R_{err1}(t)$ is not small enough to consider the optical signal nulled, then a second linear nulling estimate can be made based on the leftover error signal. The total estimate to cancel the optical signal in the second iteration is:

$$\Delta H_2(t) = \Delta H_1(t) - (L_o - R_1)\frac{H_1 - H_o}{R_1 - R_o} f_h(t - \frac{\Delta\varphi_L}{\omega_o} + \frac{\Delta\varphi_h}{\omega_o}) \qquad (5)$$

which is the sum of the first nulling estimate and an incremental adjustment based on the new local slope $(R_1\text{-}R_o)/(H_1\text{-}H_o)$. The new heater signal $\Delta H_2(t)$ is now applied with the optical signal,

and the net response of the thermistor is measured. The total response is the second error signal $\Delta R_{err2}(t) = \Delta R_{opt}(t) + \Delta R_2(t)$, where is $\Delta R_2(t)$ is thermistor response to the $\Delta H_2(t)$ heater signal by itself. If $\Delta R_{err2}(t)$ is small enough to consider the optical signal nulled (e.g., < 1 % of $\Delta R_{opt}(t)$), then $\Delta H_2(t)$ provides the electrical substitution measured power, otherwise the iterative nulling procedure continues. For FTS measurements based upon this method, it typically takes 3 iterations to reach cancellation at the 99 % level. A graphical illustration of this iterative procedure is shown in the Supplementary Material section, in Figures S1-S6. There is a limit to how perfectly cancellation can be achieved: at each subsequent iteration the power differences are smaller and thus the linear approximation for response is more accurate, but with smaller power differences comes lower signal-to-noise in the thermistor measurement. Noise in the amplitude and phase of the measured thermistor resistance will impact how well the heater feedback will match the optical signal for cancellation.

Once the nulling of the optical signal has been accomplished, it is straightforward to calculate the electrical substitution power which was required. The "feedforward" power used for nulling the optical signal is the power contained in the $\Delta H_n(t)$ signal, if the iterative procedure is carried to the nth step. The instantaneous differential power signal is calculated directly from the monitored heater voltage and the heater current (from voltage measured across a precision resistor in series with the receiver heater), i.e., $\Delta H_n(t) = I_n(t)V_n(t)$. The average power over a period is:

$$\overline{\Delta H_n(t)} = \frac{1}{T}\int_0^T I_n(t)V_n(t)dt \qquad (6)$$

The average can also be taken over many cycles of period T to improve signal-to-noise. For a 50 % duty cycle square wave, $\overline{\Delta H_n(t)} = \frac{\pi - \varphi}{2\pi} I_{n0}V_{n0}$, where φ is the phase difference between the current and voltage signals and I_{n0} (V_{n0}) is the amplitude of the heater current (voltage) in the nth step. In the sinusoidal case, $\overline{\Delta H_n(t)} = \frac{1}{2} I_{n0}V_{n0}\cos\varphi = I_{rms}V_{rms}\cos\varphi$. Typically, the impedance will be exclusively resistive and φ will be nearly zero.

In addition to this feedforward power, the additional error signal needs to be included. The error signal is small, so is well-approximated by a linear resistance-to-power relationship. The magnitude of this additional contribution is given by:

$$\Delta P_{lin} = (L_o - R_n)\frac{H_n - H_{n-1}}{R_n - R_{n-1}} \qquad (7)$$

where $H_i(R_i)$ is the power (resistance) of the ith feedforward iteration and the nth iteration is close enough to nulling the optical signal that the resistance error signal is in the linear regime. If $\Delta P_{lin} < 0$, then the feedforward power is too large and the linear leftover corrects this overshoot, and if $\Delta P_{lin} > 0$ then the feedforward power is slightly too small.

3. Procedures for Generalized Electrical Substitution (ES)

We will discuss three specific examples where generalized electrical substitution can be used to make absolute power measurements: Fourier-transform spectroscopy, arbitrary periodic signals, and noisy periodic signals. Each case is an example of a practical measurement situation where NIST has been challenged to make absolute power measurements, and where standard electrical substitution techniques do not suffice. The case of Fourier-transform spectroscopy with electrical substitution (ES-FTS) will be described in detail, and the other two examples are similar so will only be summarized briefly.

3.1. Fourier-Transform Spectroscopy with ES

Fourier-transform (FT) spectroscopy can enable high resolution spectral calibration of absolute power with ACRs, as long as the electrical substitution method can be applied to the interferometric waveforms produced by FT spectrometers. Spectral measurements with ACRs are possible using monochromators, but FTIR spectroscopy with fast ACRs would enable faster scans with higher spectral resolution and better signal-to-noise. Step-scan FTIR spectroscopy can also be used with ACRs for spectral measurements, but step-scan mode generally exhibits higher noise than continuous-scan FTIR spectroscopy in commercial instruments. We will outline the procedures compatible with continuous-scan FTIR spectroscopy at frequencies commensurate with the inverse of the ACR time constant. The description here will be complementary to that contained in another one of our papers, which provides a more complete mathematical description, as well as details of the ES-FTS electronics hardware and software [17].

The procedure can be best understood by analogy with the single frequency procedure described in Section 2.2.2, with FT mathematical techniques employed to carry out multiplexed data analysis and feedforward calculations at all frequencies at the same time. It is assumed here that the optical signal incident on the detector comes from a source modulated by a Michelson interferometer in continuous-scan mode. The iterative multiplexed feedforward procedure for electrical substitution includes the following specific steps:

1) *Test Pulse Heater Signal:* With optical signal blocked, apply a test heat pulse with broad spectral character; the heat pulse should have frequency components with span the electrical frequency range required to characterize the entire wavelength range of interest. We typically use a heat pulse with the shortest duration possible using our electronics, which is about 10 μs. The Fourier transform of such a pulse has significant amplitude over the full spectral range up to about 100 kHz. In an interferometer, there is constructive interference whenever the path difference δ between the moving and fixed mirrors is an integral multiple of the wavelength (i.e., $\delta = \lambda n$). The path difference changes by $2V$ per second, where V is the velocity of the moving mirror, so there are $2V/\lambda$ periods of the modulated signal ("fringes") per second. The scan frequency of an interferometer is defined $f_{scan} = \frac{2V}{\lambda_{HeNe}}$, where λ_{HeNe} is the wavelength of the metrology laser, usually a helium-neon type. For any other wavelength λ, the associated fringe frequency (the corresponding frequency of the electrical signal from the detector) is

$f_\lambda = \frac{2V}{\lambda} = f_{scan} \cdot \frac{\lambda_{HeNe}}{\lambda}$. Therefore, for a 100 Hz scan frequency (and λ_{HeNe} = 633 nm), the wavelength range 1 μm to 30 μm corresponds to the electrical frequency range 63.3 Hz to 2.11 Hz.

The test pulse and the thermistor's response to it are recorded, and these data are used to compute the transfer function required to estimate the nulling signal. This feedforward transfer function contains amplitude and phase information at all frequencies associating heating of the bolometer with thermistor response, and can be considered a gain function between applied heater voltage and change in thermistor voltage. This gain function can be computed from the measured thermistor voltage response according to [17]:

$$G(\sigma) = \frac{\mathscr{F}(h_m(\delta))}{\mathscr{F}(h_{app}(\delta))} \tag{8}$$

where δ is the optical path difference, σ is the spectral parameter of the FT spectrometer in units of wavenumber, $h_{\mathrm{app}}(\delta)$ is the applied heater voltage, $h_m(\delta)$ is the measured thermistor voltage change, and $\mathscr{F}$ is the Fourier transform of the referenced function.

2) *Open Loop Optical Signal:* Measure the bolometer response with no electrical heater signal applied. This response is a thermistor voltage interferogram, which will be denoted $b_m(\delta)$.

3) *First Interferogram Estimate for Nulling:* Use a linear approximation for estimated heater power based on the test signal response, with the amplitude and phase shift for each frequency determined from $G(\sigma)$. The first estimate for the nulling interferogram $h_1(\delta)$ to apply to the heater is given by:

$$h_1(\delta) = -(b_m * g_{-1})(\delta) = -\int_{-\infty}^{\infty} b_m(\delta) g_{-1}(\delta - \delta')\, d\delta' \tag{9}$$

$$\text{where } g_{-1}(\delta) = \mathscr{F}^{-1}\left(\frac{1}{G(\sigma)}\right)$$

4) *Response with Nulling Interferogram Applied:* The heater first estimate interferogram is now applied together with the optical signal, and the net response from the thermometer is measured. The response is the first error signal, the difference between the first approximation for nulling and the measured result.

5) *Continue Iterating:* If the first error signal is not small enough to consider the optical signal nulled, then a second linear nulling estimate can be made based on the leftover error signal. In this iteration, the optical signal used as a starting point in Step 2 above is the first error signal, from Step 4 of the first iteration. The heater estimate calculated from Equation 9 in this iteration can be labeled $h_2(\delta)$, and the total applied heater voltage in Step 4 during this iteration will be $h_1(\delta)+h_2(\delta)$. This process of iteration can be repeated until the amplitude of the error signal is small enough to consider the optical signal nulled by the heater interferogram.

Once nulling of the optical signal has been accomplished, the electrical substitution power can be determined from measurements of the heater current and voltage interferograms. The feedforward power used for nulling the optical signal is the power contained in the $h_1(\delta)+\ldots+h_n(\delta)$ signal, if the iterative procedure is carried to the nth step. The power can be computed using:

$$P(\sigma) = \frac{1}{T_w(\sigma)A(\sigma)} \mathscr{F}\left(\left[\frac{V_{ref}(\delta)}{R_{ref}} \right] [V_h(\delta)] \right) \tag{10}$$

where $V_h(\delta)$ is the interferogram of applied voltage to the heater, $V_{ref}(\delta)$ is the interferogram of voltage across the precision reference resistor in series with the heater, R_{ref} is the resistance of the precision reference resistor used to determine current through the heater, $A(\sigma)$ is the spectral absorptance of the bolometer absorber, and $T_w(\sigma)$ is the spectral transmittance of the cryostat window. In addition, one can account for the small offset power indicated by the error signal, by including its contribution assuming a linear power-resistance relationship for the small signal limit. As typical for FT spectrometer measurements, the closed-loop measurements (optical signal + heater feedforward drive) can be averaged for many measurement scan cycles in order to achieve higher signal-to-noise.

3.2. Electrical Substitution for Arbitrary Periodic Signals

The generalized ES method can be used to determine the absolute power in arbitrary periodic optical signals. For instance, as described earlier, a chopped signal incident on a detector can differ significantly from square wave if the beamspot is large or if the geometry or motion of the chopper is non-uniform. Assuming a square wave incident signal could lead to significant error, but the generalized ES method can account for the exact shape of the waveform, just as it can account for the shape of an interferogram output of an FT spectrometer. The steps are the same as for ES-FTS: 1) the heater test pulse determines the gain function (amplitude and phase) for each sinusoidal frequency component; 2) the open loop signal is measured to determine what frequency components are present in the incident beam; 3) using Equation 9, the feedforward heater contribution is determined; 4) the net response to optical and feedforward signals is measured; and 5) the process is iterated using this net "error" signal as a starting point if the first-estimate nulling error is considered too large.

3.3. Electrical Substitution for Noisy Periodic Signals

Another situation where generalized ES can be useful for absolute power calibration is for noisy periodic source signals. For instance, consider the case where one needs to calibrate the output of a pulsed laser, where the pulse rate is relatively slow (on the order of 1 Hz to 1 kHz) and there is significant pulse-to-pulse variation in the power (1 % - 5 %). Lasers with pulse rates on the order of MHz appear to be nearly continuous-wave even for fast ACRs, but for slow pulse rates, the ACR may integrate over only a few source periods during its relaxation time.

Similar to the ES-FTS and arbitrary period signal cases, one characterizes the bolometer spectral gain function with a heater test pulse. One also characterizes the optical signal in open-loop mode, but to get the mean response one must average over many pulses because there is significant variation between pulses. The correct feedforward heater contribution is determined from the mean optical signal response using Equation 9, but the iterative procedure is not useful because it cannot reduce the pulse-to-pulse variation effect. Instead, the leftover signal, which could be as large as several percent, can be recorded and converted to a power estimate in linear approximation. Given that this error signal is much reduced from the original signal, this small-signal approximation will often be valid. Adding the power in the feedforward signal and this leftover signal provides a calibration of pulse trains from the laser, where the uncertainty can be significantly lower than its pulse-to-pulse variation. The feedforward signal power by itself provides a calibration of the mean power of the laser over many pulses. The leftover signal provides data on the average laser power variation and also could be used to monitor power variation over time.

4. Detectors for Generalized Electrical Substitution (ES)

4.1. Introduction to ES Detectors

Appropriate electrical substitution radiometers (ESR) must be coupled with the ES methods in order to perform absolute calibrations of optical power. The new generalized ES methods place additional requirements on the properties of optimized ESRs. First, the "generalized" ESRs must be up to 1000 times faster in response compared to ACRs, which typically exhibit time constants between 1 and 10 seconds. Second, optical/electrical non-equivalence must be maintained in dynamic measurements, not just for DC equilibrium measurements.

As described in the introduction, we have chosen to develop planar bolometric radiometers (PBRs) as the route to enable much faster ACRs. By transitioning from the three dimensional hand-assembled ACR designs of the past to planar, thin film designs, miniaturization is simplified and manufacturability is markedly improved. Detector time constants roughly scale with device volume (for equivalent thermal link thermal conductance), so miniaturization enables time constants better than 1000 times faster than legacy ACRs (for equivalent power sensitivity). PBRs made using standard microelectronic techniques for thin film fabricated devices can be manufactured with tens or even hundreds of identical detectors on a single wafer, accelerating testing and potentially improving reproducibility.

4.2 Detector Designs

In this work we have tested and developed two types of PBRs, both of which have planar absorbers with near-unity absorptivity over a significant infrared spectral range. These cryogenic devices can have noise floors less than 1 nW and measure powers up to approximately 1 mW. The first type of detector is a "one-off" gold-black PBR on a sapphire substrate with custom thermistor and heat link integrated into the device by hand [13]. This device has a time constant of approximately 23 ms at a temperature near 6 K and has been used to verify the accuracy of the ES-FTS method and electronics for optical power calibrations.

The second type of device under development is a fully microfabricated carbon-nanotube PBR on a micromachined silicon substrate, with integrated thin film thermistor and heater. PBRs of this type have been well-described in a series of recent papers [14,18,19], and a general schematic is shown in Figure 7. Time constants for devices of this type have been measured to be as small as 12 ms at 6 K, and could be significantly less in future planned designs.

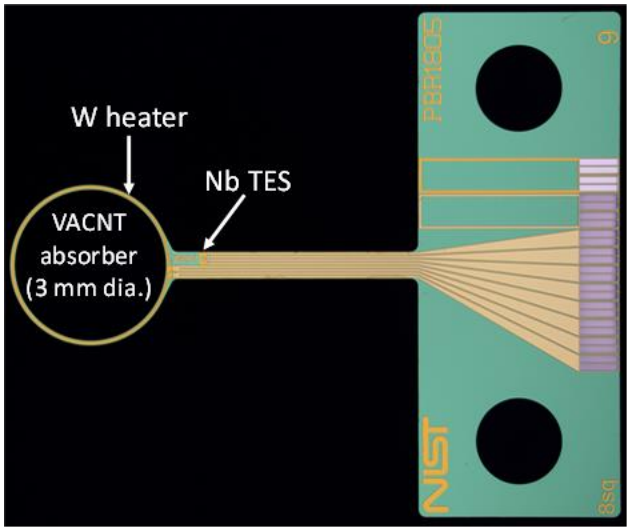

Figure 7. Image of a PBR with an absorber composed of vertically-aligned carbon nanotubes used in this study.

Most recently, we have fabricated and tested a carbon nanotube PBR design with the following specific attributes: superconducting niobium (Nb) thermistor, tungsten (W) heater, vertically-aligned carbon nanotube (VACNT) absorber, and superconducting vanadium (V) wiring, all deposited on a micromachined silicon substrate. The thermistor is a transition edge sensor (TES), i.e., when operated midway into the superconducting transition it exhibits very high temperature sensitivity. The superconducting wiring eliminates Joule-heating effects along the length of these leads, localizing heating to the thin film tungsten heater. The thermal conductance between the receiver and heat sink of the PBR is determined by the length and width of the silicon neck between the absorber "head" and the base of the device. We have fabricated a range of neck form factors between 5:1 and 24:1, which can be used to tune the response time and sensitivity for this type of device.

4.3. Experimental Results

The electrical and optical measurements on these two types of PBRs demonstrate their applicability and promise for integration with generalized electrical substitution. The PBR which has been thoroughly tested so far with our electronics for ES-FTS is the gold-black detector, and it has demonstrated agreement with another calibrated reference detector in a spectral calibration of optical power. We have successfully demonstrated the generalized electrical substitution method with FTS, achieving uncertainty in detector response of 0.13 % (k=1) and total measurement uncertainty of 1.1 % (k=1) in the mid-infrared for spectral optical

power calibrations [17]. Figure 8 shows the quality of spectral cancellation by the generalized ES method: the leftover signal in "closed loop" mode is less than 1 % of the "open loop" optical

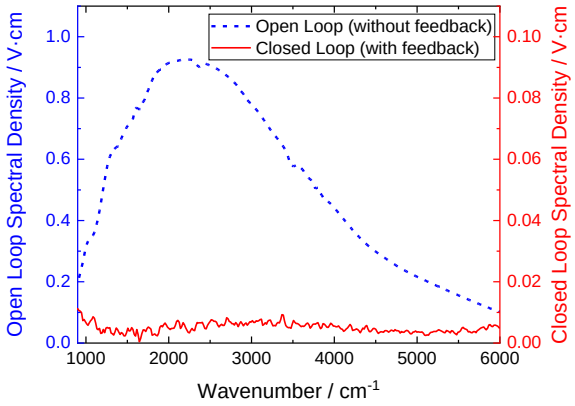

Figure 8. Spectral cancellation achieved by electrical substitution with a Fourier-transform spectrometer (ES-FTS). The closed loop signal with electrical feedback is < 1 % of the peak open loop signal (scale for closed loop is 10x magnified from the open loop range).

signal. The effect of noise on the analysis procedure and how noise limits the ability to completely cancel the signal and minimize the leftover signal is an active area of continuing research. The detector spectral responsivity system used to acquire these data is shown in the Supplementary Material, in Figure S7. At the same time we have been testing and optimizing wafers of PBRs with vertically aligned carbon nanotube absorbers (VACNT PBRs), which promise to have superior properties for this application: faster response time, wider spectral coverage with near-unity emissivity, and full microfab manufacturability.

A number of recent experiments have demonstrated that the cryogenic VACNT PBRs attain good optical/electrical non-equivalence and high absorptivity from near-infrared to far-infrared. Figure 9 shows an intercomparison of a VACNT PBR with a legacy NIST ACR,

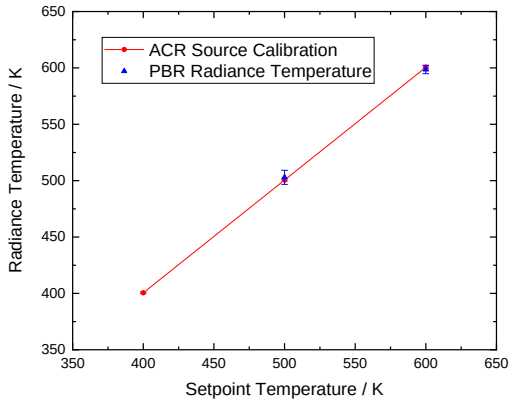

Figure 9. Intercomparison of a VACNT PBR and legacy ACR measuring an infrared blackbody source at different core setpoint temperatures, demonstrating agreement within uncertainties.

showing agreement within uncertainties for broadband optical power. The reflectance of the type of VACNT absorber used here has been measured over the range from approximately 400 nm to 400 µm, demonstrating total hemispherical reflectance in the 0.1 % range from 400 nm to 50 µm and specular reflectance ≤ 2 % at wavelengths as long as 394 µm [14,20,21].

Optimizing the VACNT PBRs for sensitivity and speed, we have developed an integrated thin film Nb thermistor with a large temperature coefficient of resistance (TCR) and have chosen

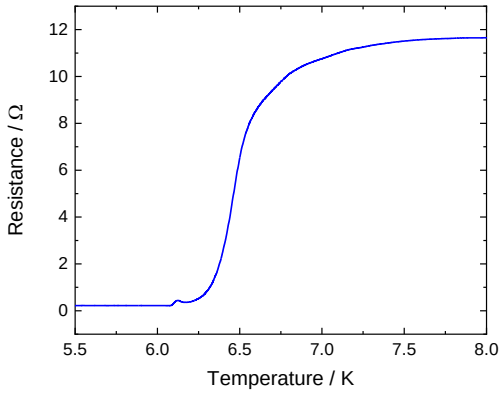

Figure 10. Superconducting transition of the Nb thin film thermistor of a working VACNT PBR. Operated at a temperature of 6.46 K, unitless sensitivity α (=$T/R \cdot dR/dT$) is greater than 50.

a thermal conductance for the thermal link to achieve time constants near 10 ms. The Nb thermistor superconducting transition for a working VACNT PBR detector is shown in Figure 10. The TCR (=$1/R \cdot dR/dT$) in this case is about 8.64 K^{-1} and the unitless sensitivity α (=$T/R \cdot dR/dT$) is 55.8 near the center of the superconducting transition at 6.46 K. Typical values of α for germanium resistance thermometers, often used in legacy ACRs, are around 10 times

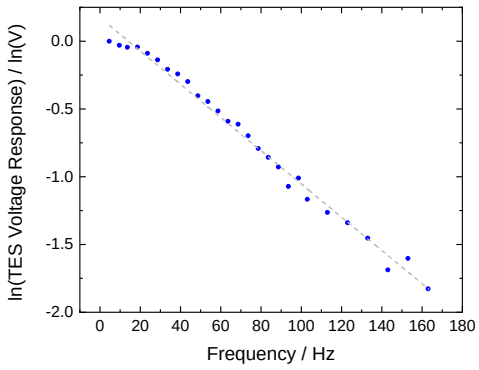

Figure 11. Signal falloff for a VACNT PBR as a function of chopper frequency. The signal is the voltage output from the Nb transition edge sensor (TES) thermistor. Fitting the natural logarithm of the signal with a straight line implies a time constant of about 12 ms.

less sensitive (α ~5). By chopping the optical signal incident on the detector over a range of frequencies, it is possible to extract the optical time constant for the detector. Falloff of the measured signal amplitude with frequency is plotted in Figure 11, and the fitted decay frequency is f_o=81.54 Hz, indicating a time constant of $1/f_o$ = 12.3 ms. The effects of chopping speed, as described in Section 2.2 are clearly exhibited in Figure 12. At 9.6 Hz the response from the Nb TES thermistor is relatively square, at 43.6 Hz is reduced in size but still shows some sign of saturation, and by 78.6 Hz has about 45 % the original amplitude and looks triangular.

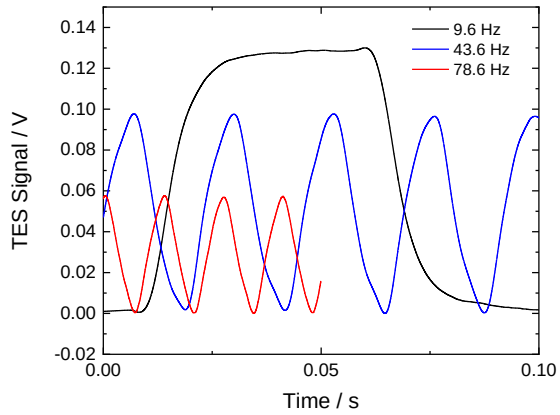

Figure 12. Time dependence of the VACNT PBR response, shown for three chopper frequencies (black = 9.6 Hz, blue = 43.6 Hz, red = 78.6 Hz). The signal is the voltage output from the Nb transition edge sensor (TES) thermistor. The waveform shows the expected evolution from nearly square wave to triangular.

5. Conclusions

We have developed methods and detectors for generalized electrical substitution, along with the digital electronics hardware and software required for these measurements. The basic method can determine the electrical feedback equivalent to the time-dependent optical signal incident on an electrical substitution radiometer, and the digital electronics provide the feedback in real-time to "cancel" the optical signal. The method and electronics have been validated using a gold black electrical substitution bolometer, and we are developing carbon nanotube electrical substitution bolometers with superior properties and manufacturability.

In future work we plan to continue developing faster and more sensitive VACNT PBRs and will rigorously test them when used with generalized electrical substitution. In particular, we will carefully quantify optical/electrical non-equivalence for this type of detector as a function of frequency. Further research will also be directed toward making the generalized electrical substitution method more robust in the presence of detector noise. The new method and detectors will empower researchers to conduct their own SI-traceable optical power calibrations directly against a primary standard detector for a wide variety of optical applications.

6. Acknowledgements

This work was supported in part by Air Force Metrology and Calibration Division (AFMETCAL) as part of the Calibration Coordination Group (CCG), project CCG-661.

References

1. K. Angstrom, "The quantitative determination of radiant heat by the method of electrical compensation," Physical Review **1**, 365 (1894).

2. F. Kurlbaum, "Notiz über eine Methode zur quantitativen Bestimmung der stahlenden Wärme," Annalen der Physik **287**, 591 (1894).

3. R.J. Phelan, Jr., and A.R. Cook, "Electrically Calibrated Pyroelectric Optical-Radiation Detector," Applied Optics **12**(10), 2494-2500 (1973).

4. J. Geist and W.R. Blevin, "Chopper-stabilized null radiometer based upon an electrically calibrated pyroelectric detector," Applied Optics **12**(11), 2532-2535 (1973).

5. J.E. Martin, N.P. Fox, and P.J. Key, "A cryogenic radiometer for absolute radiometric measurements," Metrologia **21**, 147-155 (1985).

6. F. Hengstberger, *Absolute radiometry : electrically calibrated thermal detectors of optical radiation* (Academic Press, 1989).

7. C.A. Hamilton, "Josephson voltage standards," Review of Scientific Instruments **71**(10), 3611-3623 (2000).

8. B. Jeckelmann and B. Jeanneret, "The quantum Hall effect as an electrical resistance standard," Reports on Progress in Physics **64,** 1603–1655 (2001).

9. T.J. Quinn and J.E. Martin, "A radiometric determination of the Stefan-Boltzmann constant and thermodynamic temperatures, between −40 °C and +100 °C," Philos. Trans. R. Soc. Lond. A **316**(1536), 85–189 (1985).

10. R.U. Datla, K. Stock, A.C. Parr, C.C. Hoyt, P J. Miller, and P.V. Foukal, "Characterization of an absolute cryogenic radiometer as a standard detector for radiant power measurements," Applied Optics **31**, 7219 (1992).

11. S.I. Woods, T.M. Jung, G.T. Ly, and J. Yu. Broadband Emissivity Calibration of Highly Reflective Samples at Cryogenic Temperatures, Metrologia **49**, 737 (2012).

12. The acronym ACR is shared by another earlier radiometer, known as an active cavity radiometer. The active cavity radiometer was not a cryogenic instrument, but it did use electrical substitution for absolute measurements of optical power. See, for instance: R.C. Willson, "Active cavity radiometer," Applied Optics **12**(4), 810-817 (1973).

13. J.P. Rice, "An electrically substituted bolometer as a transfer-standard detector," Metrologia **37**, 433-436 (2000).

14. N.A. Tomlin, M. White, I. Vayshenker, S.I. Woods and J.H. Lehman, "Planar electrical-substitution carbon nanotube cryogenic radiometer," Metrologia **52**, 376-383 (2015).

15. C.A. Hamilton, G.W. Day, and R.J. Phelan, Jr., *An electrically calibrated pyroelectric radiometer system*, NBS Technical Note 678 (National Bureau of Standards, 1976).

16. Earth Observing System SOlar Radiation and Climate Experiment (EOS SORCE) white paper, "Algorithm theoretical basis document" (Laboratory for Atmospheric and Space Physics, 2000). https://eospso.nasa.gov/sites/default/files/atbd/ATBD-SOR-01.pdf

17. J.E. Neira, S.I. Woods, J.E. Proctor, J.P. Rice, "Development of Electrical Substitution Fourier Transform Spectrometry for Absolute Optical Power Measurements," Optics Express **29**(23), 37314 (2021).

18. N.A. Tomlin and J.H. Lehman," Carbon nanotube electrical-substitution cryogenic radiometer: initial results," Optics Letters **38**(2), 175-177 (2013).

19. N.A. Tomlin, C.S. Yung, Z. Castleman, M. Denoual, G. Drake, N. Farber, D. Harber, K. Heuerman, G.Kopp, H. Passe, E. Richard, J. Rutkowski, J. Sprunck, M. Stephens, C. Straatsma, S. Van Dreser, I.Vayshenker, M.G. White, S.I. Woods, W. Zheng, and J.H. Lehman, "Overview of microfabricated bolometers with vertically aligned carbon nanotube absorbers", AIP Advances **10**, 055010 (2020).

20. C.J. Chunnilall, J.H. Lehman, E. Theocharous, A. Sanders, "Infrared hemispherical reflectance of carbon nanotube mats and arrays in the 5–50 μm wavelength region," Carbon **50**, 5348-5350 (2012).

21. J. Lehman, A. Steiger, N. Tomlin, M. White, M. Kehrt, I. Ryger, M. Stephens, C. Monte, I. Mueller, J. Hollandt, and M. Dowell, "Planar hyperblack absolute radiometer," Optics Express, **24**(23), 25911-25921 (2016).